Desalination and Water Treatment
www.deswater.com
doi: 10.5004/dwt.2020.25676

193 (2020) 11–18
July

Evaluation of capacitive deionization desalination technology for irrigation

Moustafa Elshafei*, Abdalrahman M. Amer, Ashraf Seleym, Ziad Khalifa, Tamer S. Ahmed

Zewail City for Science and Technology, British University, Egypt, Tel. +20 100 424 1056; email: moelshafei@zewailcity.edu.eg (M. Elshafei)

Received 6 December 2019; Accepted 12 February 2020

ABSTRACT

Desalination of brackish groundwater has great potential to alleviate the problem of the limited water resources in Egypt. In this paper, we studied the desalination of brackish water for irrigation purposes using capacitive deionization (CDI) technology. We investigated a modular unit for use in greenhouses (GH). A GH for the production of tomato requires about 3.2 m^3/d of water. The target CDI unit has a production capacity of 32 m^3/d for irrigation of 10 greenhouses from brackish water. The paper provides an extensive simulation study to illustrate the influence of various design parameters and to unveil the CDI technology pros and cons and its inherent limitations. Although the CDI unit provides comparable energy consumption to typical reverse osmosis units, it does not require frequent replacement of membranes, and the activated carbon can easily be manufactured using local material.

Keywords: Desalination; Capacitive deionization; CDI; Activated carbon; Porous materials; Salt ionization; Electrostatic double layer; Electrostatic ion separation

1. Introduction

Freshwater scarcity is one of the most challenging problems facing the world today. Around 75% of the Earth's surface is covered by water. However, out of which, 97.5% is in the form of oceans. While rivers, lakes, and surface ice represent only 1.2% of the freshwater sources on earth [1]. According to UN FAO [2], it is estimated that by 2025, 1,800 million people will be living in countries or regions with absolute water scarcity, and two-thirds of the world population could be under stress conditions [2]. Freshwater scarcity is a serious issue. It slows or stops the economic growth of a country, reduces agricultural output, deteriorates public health, and quality of life. UN has called for global action to ensure sustainable development of human beings, where water comes as the six-goal in the UN sustainable development goals [3,4].

As an example, the Egyptian quota from the Nile River is limited to 55 billion m^3/y and is expected to decrease due to the increasing demand for water by other Nile basin countries. According to an Egyptian government report [5], the total population of Egypt increased from 22 million in 1950 to around 85 million in 2010 (currently, it reached about 99.4 million). This increase in population growth will continue for decades to come and it is likely to increase to between 120–150 million by 2050. Egypt has reached a state where the quantity of water available is imposing limits on its national economic development. As an indication of water shortage, the threshold value of 1,000 m^3/cap/y is usually used as an indicator. Egypt has already gone below this threshold since the nineties, and it is expected to cross the threshold of the absolute scarcity of 500 m^3/cap/y by 2025. Due to the steady decline of the water/capita in Egypt, the government has embarked on massive strategic projects to secure freshwater by seawater desalination. On the other hand, the majority of aquifer systems in Egypt contain large quantities of untapped brackish water. Desalination of brackish water could provide an economic solution via

* Corresponding author.

Presented at the 4th International Water Desalination Conference: Future of Water Desalination in Egypt and the Middle East, 24–27 February 2020, Cairo, Egypt

small to medium distributed units. The problem of water scarcity is particularly critical in most of the Middle East and North Africa (MENA) countries. It is expected that by 2025 at least 10 MENA countries will be under the absolute water scarcity level of 500 m^3/cap/y.

As such, there is a growing need in Egypt and other MENA countries to explore desalination technologies to meet their growing need for freshwater. Several water desalination technologies are currently used based on the utilization of thermal energy, mechanical energy, and electrical energy [6]. The most widely used processes for desalination include membrane separation systems: reverse osmosis (RO), and electro-dialysis (membrane process, where the driving force is the potential applied between the two electrodes); and thermal separations including multi-stage flash distillation (MSF), multi-effect distillation and mechanical vapor compression. Among these processes, RO and MSF methods are employed in the bulk of the plants (90%) to desalinate seawater worldwide. Today, RO, [7] is the leading technology for new desalination installations, with over 80% share in the over 15,000 desalination plants installed worldwide, mainly because of its less energy consumption, 3–8 kWh of electric energy per m^3 of freshwater produced from seawater, compared to thermal desalination, and because of the continued improvements in membranes technologies. However, the large scale use of RO technology has created a serious membrane disposal problem. Capacitive deionization (CDI) is an emerging technology [8–10], which can be directly driven by solar power [11]. Unlike conventional thermal/mechanical desalination methods, which separate water from salts, the CDI method separates the salt, in the form of ions, from the water stream using electrostatic forces. CDI is low pressure and low-temperature process [8,9]. The ions are removed from water rather than water from the ions. It requires a small voltage of 1.2–1.5 volts for desalination. Electrode cleaning is achieved by short-circuiting the electrodes of a CDI cell, with no special chemicals to clean the electrodes. During the discharging step, the energy stored in the electrical double layer (EDL) capacitors [10] can be recovered and used to charge a neighboring CDI cell or a battery [12]. The energy consumption of CDI is less compared to other desalination technologies [9]. In particular, CDI is potentially more energy-efficient for brackish water desalination [13,14].

2. Capacitive deionization

In the CDI systems, saline water is made to pass between a pair of porous electrodes connected to a voltage source, as shown in Fig. 1. A CDI is a two-step process [8,10], the first step is ion adsorption or charging that results in a pure permeate stream where ions are adsorbed in porous charged electrodes. As the voltage is applied to the electrodes, the positive ions, cations, move to the cathode, and anions move towards the anode. Two layers of opposite polarity are formed at the electrode-solution interface which is referred to as an EDL and ions are stored in these EDL's. In the next step, voltage is reversed so that the ions get desorbed and flows out of the CDI cell as a brine stream and thus cause regeneration of electrodes. CDI differs from Electrodialysis [15], in the sense that it does not need membranes. The problems of membrane fouling are not present in CDI, and since it utilizes direct electrical energy for desalination, it has the potential to be energy efficient and robust technology for water desalination.

3. Modeling of basic cell

The CDI cell in its simplest form is shown in Fig. 2. It is placed in a rectangular container made of non-conducting material, where the feed water comes to the tank when valve *V*1 is open. CDI cell contains two electrodes, each one consists of a porous material like activated carbon, and a conducting current collector.

After the container is filled, valve *V*1 is closed and a voltage *U*1 is applied at electrode *A*, and a potential –*U*1 is applied at electrode *B*. As the voltage is applied to the electrodes, due to the presence of an electrostatic field in

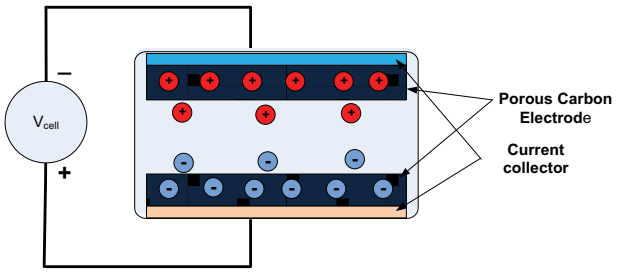

Fig. 1. Capacitive deionization.

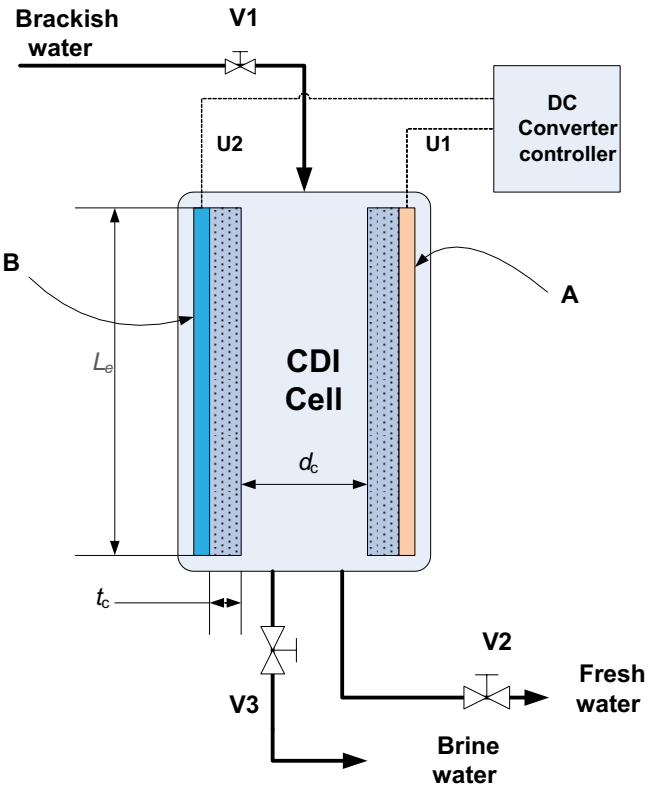

Fig. 2. Basic CDI cell.

between the electrodes, there is a movement of ions such that the positive ions, cations, move to the cathode and negative ions, anions, towards the anode, where the ions are stored in the EDLs. This charging or adsorption step results in a pure permeate in the container. In the next step, the applied voltage is disconnected and valve *V*2 is opened to discharge permeate into a freshwater tank. Next, valve *V*2 is closed and valve *V*1 is opened to refill the tank with raw water. Next step, valve *V*1 is closed and zero or reversed voltage is applied to the electrodes to force the charges in the porous electrodes to disrobe in the water. This step causes the regeneration of electrodes and results in highly saltwater in the container. Next, valve *V*3 is turned on and the highly saltwater, known as brine, is discharged into a brine tank. When the cell container becomes empty, valve *V*3 is closed, and valve *V*1 is turned on, and the cycle is repeated. The operational cycle is summarized in Table 1.

An electric circuit model during the adsorption step of a CDI cell with the two porous electrodes is shown in Fig. 3.

The right activated carbon electrode capacitance, Fig. 3, is represented by capacitor C_1, and the left electrode capacitance is represented by the capacitor C_2.

The capacitance associated with the two electrodes is equal to maintain charge balance in the solution that is, $C_1 = C_2$. R_w is the electrical resistance of the water between the two opposite electrodes and i is the current flowing in the CDI cell through the water resistance. The resistance of water is given by the Eq. (1):

$$R_w(t) = \frac{\rho_e(t) d_c}{A_c} \tag{1}$$

where A_c is the physical area of the activated carbon electrode in m^2; d_c is the distance between the activated carbon electrodes; $\rho_e(t)$ is the resistivity of the water. The resistivity of water (2) depends on temperature and concentration, and it is approximately by [16].

$$\rho_e(t) \cong \frac{5}{x(t)\left(1+\alpha_T(T-25)\right)} \tag{2}$$

where $x(t)$ is the concentration of salt in kg/m^3 (or g/L); and $\alpha_T = 0.022$/°C.

Let $A_c = L_c W_c$ be the physical area of the capacitor. The effective area of the capacitance associated with each AC electrode is given by:

$$A_e = \left(A_c t_c \rho_{ac}\right) S_{ac} \tag{3}$$

where S_{ac} is the specific surface area of the activated carbon, which is typically between 600–2,500 m^2/g, and ρ_{ac} is the density of activated carbon, t_c is the thickness of the activated carbon material. The capacitor formed by the EDL is given by Eq. (4).

$$C_{1,2} = C_e(t) = \frac{A_e \varepsilon_0 \varepsilon_r}{t_{cs}(t)} \tag{4}$$

where ε_0 is the permittivity of free space, ε_r the relative permittivity of water (78), and t_{cs} (t) is the width of the electrical double layer. The width of the EDL is of an order of nanometers.

The electrical double layer width is often approximated as Debye length using Gouy Chapman model [10]. Debye length λ_D, which is given by:

$$\lambda_D = \left[\frac{\varepsilon_0 \varepsilon_r K_B T}{2 q_e^2 C_x}\right]^{0.5} \tag{5}$$

where K_B is the Boltzmann constant, and T is the temperature in Kelvin, q_e is the electron charge, and C_x is the ionic salt charge concentration, $C_x = F \times X_m$; X_m is the molar concentration of salt mol/L, F is the Faraday constant (96,485 coulombs). At 300 K,

$$\lambda_D \cong \frac{0.304}{\sqrt{X_m}} \tag{6}$$

λ_D is in nanometer. We take $t_{cs} \cong \lambda_D 10^{-9}$ in meters. However, for a practical purpose we use $t_{cs} = \frac{\mu_D}{\sqrt{X_m}}$ where μ_D is to be determined experimentally.

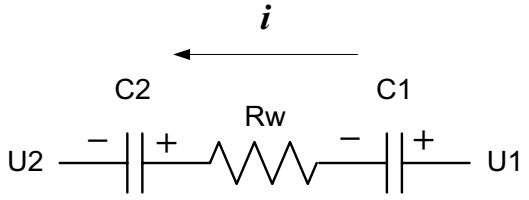

Fig. 3. Electric circuit model of a CDI cell.

Table 1
Operation steps of the basic system

Step	Operation	*V*1	*V*2	*V*3	*U*1	*U*2	Period
1	Fill the tank with raw water	On	Off	Off	Open	Open	*T*1
2	Adsorption step	Off	Off	Off	+	-	*T*2
3	Release the water to the permeate tank	Off	On	Off	Open	Open	*T*3
4	Fill the tank with raw water or recycled brine	On	Off	Off	Open	Open	*T*4
5	Desorption step	Off	off	Off	-	+	*T*5
6	Release the salty water to the brine tank	Off	Off	On	Open	Open	*T*6

Fig. 4, gives EDL width vs. concentration at 300 K for NaCl solution. For example, for seawater, EDL is about 4 A, while for brackish water at 5,000 ppm is about one nanometer.

Applying Kirchhoff's law on the electric circuits in Fig. 3, we obtain Eq. (7).

$$U_1 = v_{c1} + \mathrm{IR}_w + v_{c2} + U_2 \tag{7}$$

where v_{c1}, v_{c2} are the capacitor's voltage. When $U_2 = -U_1 = U$, The electric potential on the solution is $E = 2U_1$. E should be kept less than 1.23 volts to avoid electrolysis of water [8,10,17]. Since $C1 = C2 = C_e$, Eq. (7) can be further reduced to:

$$U(t) = v_c(t) + I\frac{R_w(t)}{2} \tag{8}$$

where $v_c(t) = v_{c1}(t) = v_{c2}(t)$. The equivalent circuit corresponding to Eq. (8) can now be represented by a simple RC circuit as shown in Fig. 5.

However, in this circuit both R_w and the capacitors are nonlinear elements of salt concentration and time-varying during adsorption and desorption as shown in the following analysis. Let the salt concentration in the CDI cell be denoted by $x(t)$, and V_w be the volume of water in the CDI cell.

3.1. Conservation of mass

The total mass of the salt in the system is given by

$$M_s = V_w x + \frac{v_c C_e}{F} M_{\mathrm{ws}} \tag{9}$$

During the adsorption step, the total mass is constant and is equal to $M_s = V_w x_f$. However, under the applied voltage, the salt ions move from the water forming positive and negative currents to charge the cation and anion EDLs.

Differentiating Eq. (9) w.r.t. time, then

$$\frac{dM_s}{dt} = 0 = V_w\frac{dx}{dt} + K\frac{d(v_c C_e)}{dt} \tag{10}$$

$$I = \frac{d(v_c C_e)}{dt} \tag{11}$$

$$V_w\frac{dx}{dt} = -KI \tag{12}$$

where $K = M_{\mathrm{ws}}/F$, and M_{ws} is the molecular mass of NaCl and F is Faraday's constant. In Eq. (12), x is in g/L, V_w in L. Eq. (12) relates the rate of salt removal to the charging current of the EDL capacitors, where the salt is removed from water in the form of ions, which are then stored in the AC capacitors. When the salt concentration changes both the water resistance and the EDL capacitance change.

$$I(t) = \frac{d(v_c C_e)}{dt} = C_e\frac{dv_c}{dt} + v_c\frac{dC_e}{dt} \tag{13}$$

Eqs. (8), (12) and (13) are the governing equations of the CDI cell during adsorption and desorption.

3.2. CDI unit for agriculture applications

We considered here a modular desalination unit for use in greenhouses (GH). A GH, typically 9 m × 40 m, for production of tomato requires about 3.2 m³/d of water. The target CDI unit has a production capacity of 32 m³/d for irrigation of 10 greenhouses by desalination of brackish water. In this section, we provide a detailed description of the CDI desalination unit.

We assume the TDS of the feed brackish water is 4,000 ppm (4 g/L). The desired TDS for water irrigation is 800 ppm. We will assume in our analysis that NaCl is the dominant salt ingredient. In this case, the Molecular weight of salt M_{ws} is taken to be 58.44g/mol. However, more accurate calculations of the M_{ws} can be obtained if the analysis of the salt species of the brackish water is known.

The cells utilize activated carbon in the form of 4 × 8 granules with bulk density between 0.45 to 0.55 g/cm³. The simulation is based on the bulk density of 0.5 g/cm³. The specific surface of the activated carbon is 900 m²/g.

The unit is to be made of Nu = 50 cells, each cell consists of two AC electrodes. The area of each electrode is

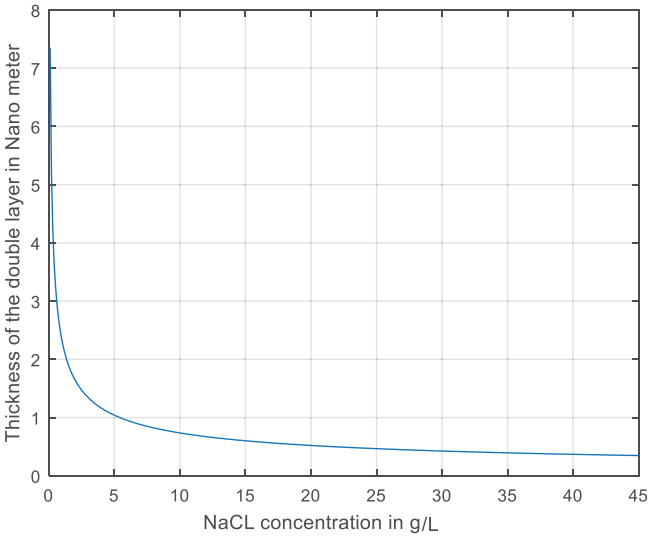

Fig. 4. EDL width vs. NaCl concentration in g/L at 300 K.

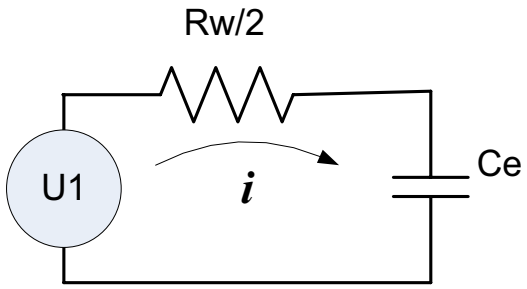

Fig. 5. Equivalent circuit of a CDI cell.

1.0 m × 1.0 m, with a graphite coated aluminum charge collector of 2 mm thickness. The AC granules are kept in a plastic screen pocket of a width of 12 mm. The electrodes are separated by water passage of width *dc* = 4 mm. The mass of the activated carbon per electrode came to 6,000 g.

The estimated solid volume of each cell is about 10 L. The 50 cells are placed in a non-conducting container of inner dimension WI = 110 cm, HI = 120 cm, LI = 170 cm. The water is kept 2 cm below the electrodes and 3 cm above electrodes. The height of the water is then Hw = 105 cm. Now subtracting solid volume from the internal volume of the container, the water capacity of the unit is 1,738 L. The cell uses 2 HP pumps, (490 L/min) for filling and discharging the unit. The pump takes approximately 3.6 min to move water in and out of the tank. The pump operates a total of 14.4 min ($T1 + T3 + T4 + T6$, Table 1) for each water desalination processing cycle,

3.3. Performance evaluation

Eqs. (8), (12), and (13) were discretized as follows using a sampling period T_s = 1.0 s

Loop:

$$q_c(t) = q_c(t-1) + T_s I_c(t-1) \tag{14}$$

$$x(t) = x(t-1) - \left(\frac{K}{V_w}\right) N_u \left(q_c(t) - q_c(t-1)\right) \tag{15}$$

Calculate $R_w(t)$ using Eqs. (1) and (2) (16)

Calculate $C(t)$ using Eqs. (4) and (5) (17)

$$V_c(t) = \frac{q_c(t)}{C(t)} \tag{18}$$

$$I_c(t) = \frac{2\left(U(t) - V_c(t)\right)}{R_w(t)} \tag{19}$$

The loop ends when the desired concentration is achieved.

Go to loop:

The initial conditions for the adsorption step where taken as follows:

At $t = 0$,

$$q_c(0) = 0;\ v_c(0) = 0;\ x(0) = x_f$$

$$U_1(t) = -U_2(t) = U(t) = 0.46$$

$$I_c(0) = \frac{2U(0)}{R_w(0)}$$

The initial values of R_w and C_e are calculated using Eqs. (1)–(4) with $x(0) = x_f$.

3.4. Simulation of the adsorption step

The simulation results of the adsorption step are shown in Figs. 6–8.

Fig. 6a shows the salt concentration in the cell as a function of time. The adsorption cycle takes 2,236 s. The adsorption cycle is terminated when the concentration reaches the desired value of 800 ppm. Fig. 6b shows the cell current. The initial current is almost 192 A/cell and decreases quickly to about 27.7 A when the concentration of salt reaches the desired level.

Although the current density (192 A/m^2), is common in many electrolysis processes, it is not recommended in the agriculture environment. The cell area can be divided into small cells to limit the peak current in every cell to 30–50 A to enable the use of low-cost circuit breakers and electric protection gears. The current could also be reduced by increasing the gap between the electrodes but will lead to higher losses and slowing the adsorption stage.

Figs. 7a and b indicate the changes in the water resistance and the EDL capacitor charge, respectively.

Fig. 7a demonstrates the fast change in water resistance with a change in salt concentration. The water resistance

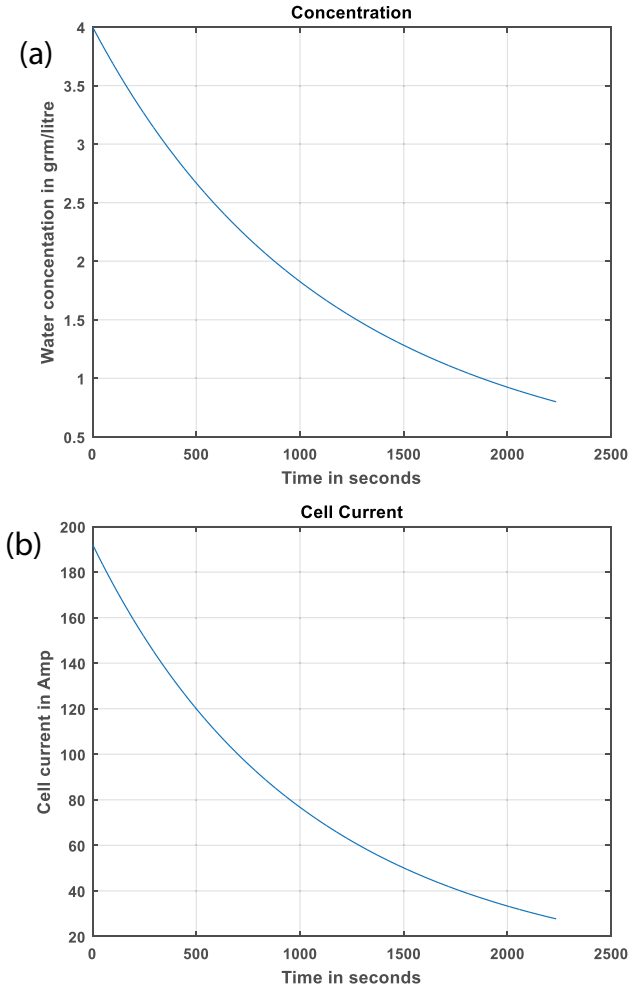

Fig. 6. (a) Cell salt concentration and (b) cell electrical current during the adsorption step.

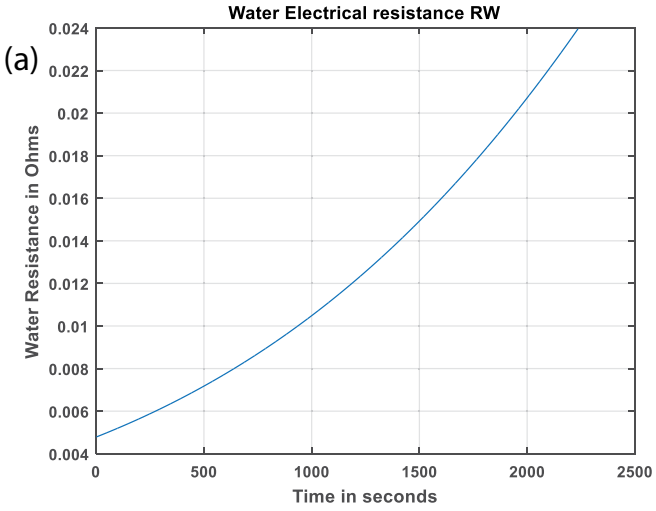

Fig. 7. (a) Water electrical resistance and (b) capacitor charge during the adsorption step.

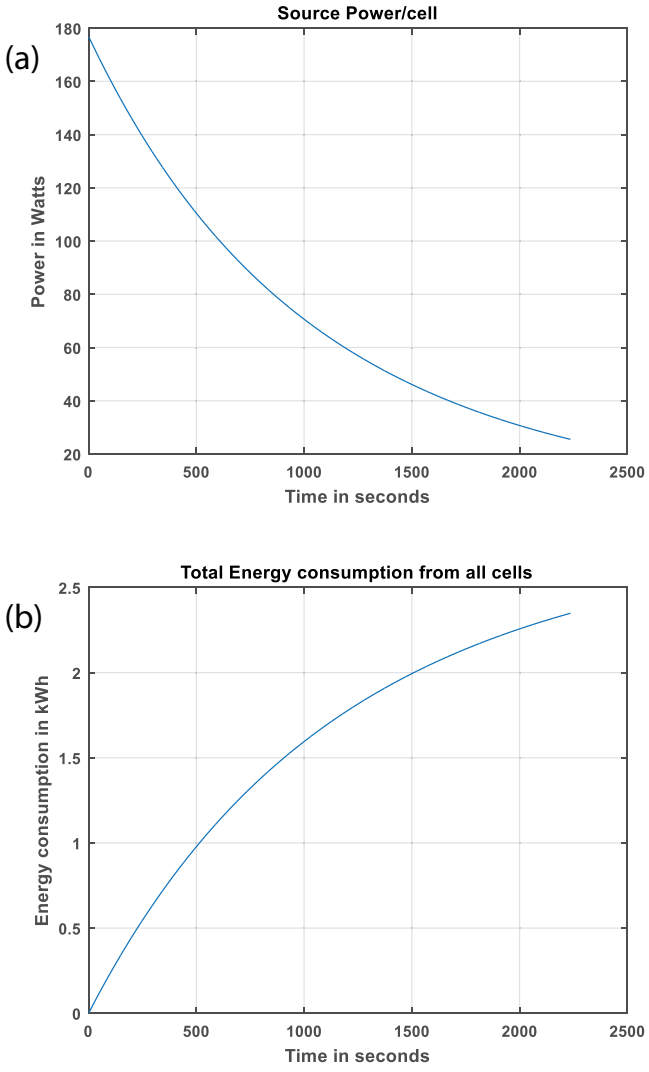

Fig. 8. (a) Source electrical power and (b) energy consumption during the adsorption step.

changes inversely with the TDS. It starts with low value at x_f = 4,000 ppm, and continue to increase as the salt concentration decreases until the end of the adsorption step.

Finally, Figs. 8a and b provide the electric power needed by the cell and the electric energy consumption during the adsorption step.

The cell power supply is required to provide a peak power of about 177 W. The total energy consumption by all cells during the adsorption step came to approximately 2.3483 kWh.

3.5. Simulation of the desorption step

The discretized Eqs. (14)–(16) were also used during discharging, with the initial capacitor charge equals to the last value at the end of the adsorption stage. When the applied voltage is taken to be zero, the EDL capacitor discharges very slowly. The discharging could take almost 8 h. The discharging rate is then assisted by applying a reverse voltage, $U1$ = –0.2 V, and $U2$ = +0.2 V.

Figs. 9 and 10 give the performance parameters during the desorption step. As illustrated in Fig. 9a, the desorption step ends when the capacitor is fully discharged and the captured ions in the EDL are release to the solution.

It is observed from Fig. 9b that the salt concentration becomes 7.2 g/L, which is the sum of the TDS of the inlet concentration, 4.0 g/L, and the salt removed during the adsorption step, 3.2 g/L. Next, Fig. 10a shows the discharge current. The negative sign indicates the current is coming out from the capacitor. The magnitude of the current increases due to the decrease in water resistance.

Although the EDL charge is zero at the end of the desorption cycle, the current reaches –150.37 A. If the control allows the adsorption step to continue, the EDL capacitors will start to store ions of the brine water.

Fig. 10b displays the power delivered by the source as a function of time. The peak power needed is about 60 W. Finally, Fig. 10c displays the total energy consumption by all the 50 cells during the desorption step. The energy consumption came to about 1.02 kWh.

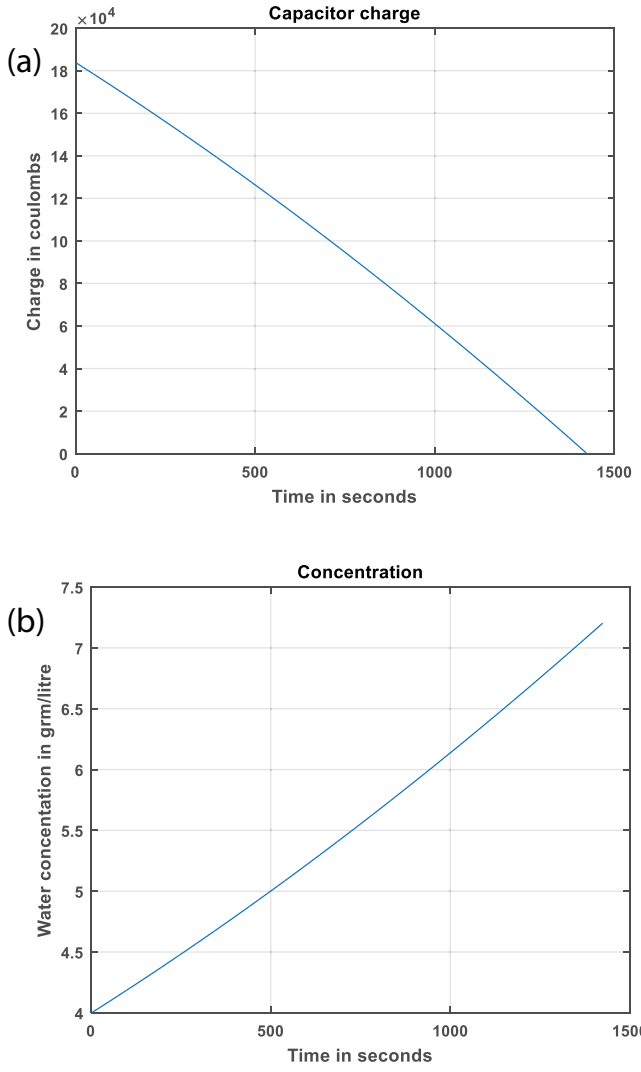

Fig. 9. (a) Discharging of capacitors and (b) salt concentration during the desorption step.

The 2 HP pump operates for 14.4 min (864 s) per process cycle, consuming 0.358 kWh per cycle.

Table 2 summarizes the complete adsorption/desorption cycle.

The adsorption/desorption cycle duration = 2,236 + 1,425 + 864 = 4,525 s. The number of cycles per day is about 19 cycles producing 33.15 m^3/d.

The total energy consumption per cycle = 2.3483 + 1.022 + 0.358 = 3.728 kWh

The water produced in one cycle = 1.736 m^3

Specific energy = 2.1476 kWh/m^3.

4. Conclusions

CDI desalination technology could provide a practical and low-cost solution for the desalination of brackish water. The paper presented a simulation study to evaluate the performance of a desalination unit for agriculture application. The proposed unit could provide irrigation water for 10 greenhouses. The CDI technology does not

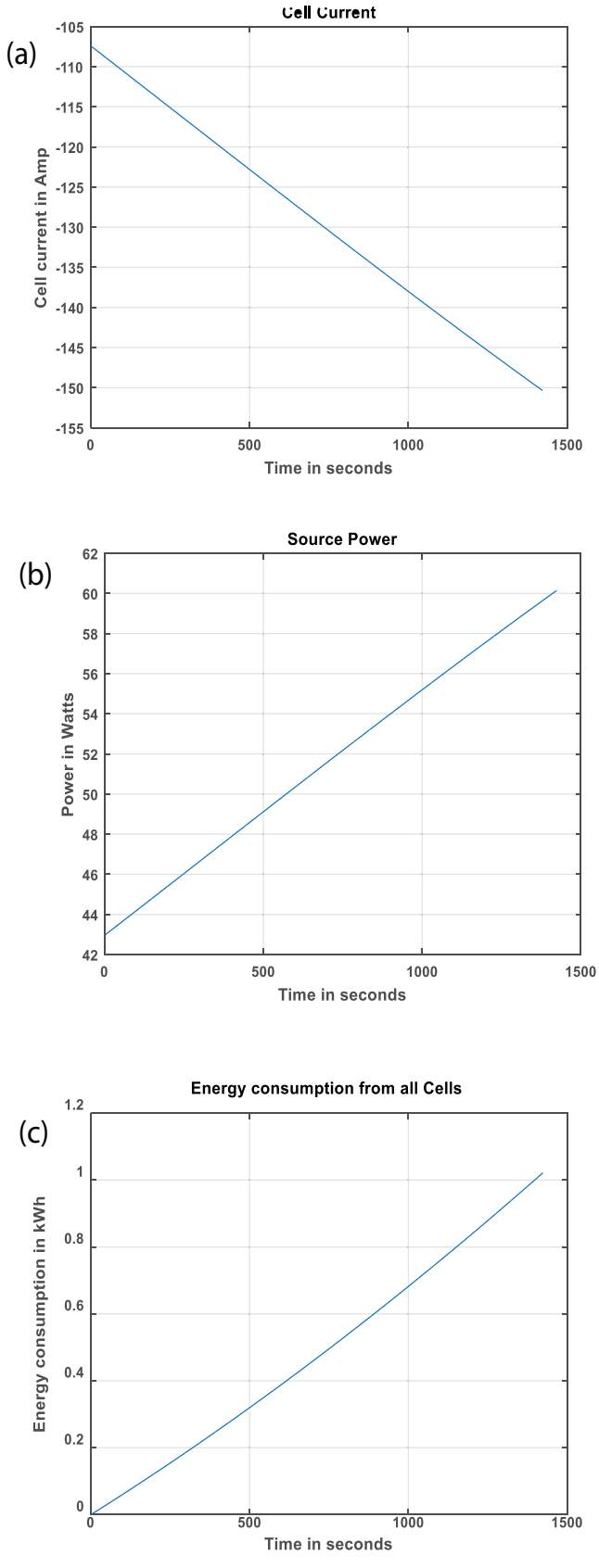

Fig. 10. (a) Cell electrical current, (b) source electric power, and (c) energy consumption during the desorption step.

Table 2
Complete adsorption/desorption cycle

Stage	Period	Energy consumption kWh
Adsorption period $T1$	2,236 s	2.1476
$T2$	3.6 min	0.0895
$T3$	3.6 min	0.0895
Desorption period $T4$	1,425 s	1.02 kWh
$T5$	3.6 min	0.0895
$T6$	3.6 min	0.0895
Total	4,525 s	3.728 kWh

use membranes and does not require special chemicals to reduce fouling as in RO. Activated carbon can be manufactured locally from agriculture waste. The paper illustrates that the desalination of brackish water using CDI technology could provide an economic solution via small to medium size distributed units. The main problem of the CDI technology is that it requires special power supplies to produce very large current at low voltage. The flow of large current is accompanied by unrecoverable energy loss in the Water. The large current flowing in the cells needs also costly electric protection and safety gear. Many operating parameters still need to be optimized to reduce energy consumption and maximize the production rate and water recovery ratio.

Acknowledgments

This work is funded by the Egyptian Science and Technology Development Fund (STDF) under US-Egypt collaboration grant number USC18- 904.

Symbols

$U1$, $U2$, U	—	Electrode voltage
ρ_e	—	Resistivity of water
A_c	—	Electrode area
d_c	—	Separation between electrodes
AC	—	Activated carbon
ρ_{ac}	—	Density of AC
R_w	—	Water resistance
Nu	—	Number of cells
C_e	—	Effective capacitance
V_w	—	Volume of water
Sac	—	Specific surface of the AC
M_{ws}	—	Molecular weight of salt
q_c	—	Capacitor charge
Ms	—	Mass of salt
x	—	Salt concentration
F	—	Faraday constant
λ_D	—	Debye length
x_m	—	Mole concentration

References

[1] P.H. Gleick, Ed., Water in Crisis: A Guide to the World's Fresh Water Resources, Oxford University Press, Oxford, United Kingdom, 1993.
[2] Food and Agriculture Organization of the United Nations, Water Scarcity. Available at: http://www.fao.org/land-water/water/water-scarcity/en/; 12, (Retrieved May 12, 2019).
[3] WWAP UNESCO, The United Nations World Water Development Report 2019, Leaving No One Behind, World Water Assessment Programme, ISBN 978–92–3-100309–7, Paris, 2019, pp. 186.
[4] UN Sustainable Development Goals. Available at: https://www.undp.org/content/undp/en/home/sustainable-development-goals.html
[5] Water Scarcity in Egypt, Ministry of Water Resources and Irrigation, Egypt, 2014. Available at: http://www.mfa.gov.eg/SiteCollectionDocuments/Egypt%20Water%20Resources%20Paper_2014.pdf
[6] A. Cipollina, G. Micale, L. Rizzuti, Eds., Seawater Desalination, Conventional, and Renewable Energy Processes, Springer-Verlag Berlin Heidelberg, 2009.
[7] J. Kucera, Reverse Osmosis, Design, Processes, and Applications for Engineers, Scrivener Publishing LLC, Mass., USA, 2010.
[8] S. Porada, R. Zhao, A. van der Wal, V. Presser, P.M. Biesheuvel, Review on the science and technology of water desalination by capacitive deionization, Prog. Mater. Sci., 58 (2013) 1388–1442.
[9] F.A. AlMarzooqi, A.A. Al Ghaferi, I. Saadat, N. Hilal, Application of capacitive deionization in water desalination: a review, Desalination, 342 (2014) 3–15.
[10] R. Zhao, Theory and operation of capacitive deionization systems. 2013.
[11] M. Elshafei1, A. Seleym, Potential of solar-driven CDI technology for water desalination in Egypt, J. Renewable Energy Sustainable Dev., 3 (2017) 2356–8569.
[12] A.M. Pernia, F.J. Alvarez-Gonzalez, M.A.J. Prieto, P.J. Villegas, F. Nuno, New control strategy of an up–down converter for energy recovery in a CDI desalination system, IEEE Trans. Power Electron., 29 (2014) 3573–3581.
[13] K. Laxmana, M. Myinta, M. Al Abric, Efficient desalination of brackish groundwater via a novel capacitive deionization cell using nanoporous activated carbon cloth electrodes, J. Eng. Res., 12 (2015) 22–31.
[14] F. Ahmad, S.J. Khan, Y. Jamal, H. Kamran, A. Ahsan, M. Ahmad, A. Khan, Desalination of brackish water using capacitive deionization (CDI) technology, Desal. Water Treat., 57 (2015) 7659–7666.
[15] A. Campione, L. Gurreri, M. Ciofalo, G. Micale, A. Tamburini, A. Cipollina, Electrodialysis for water desalination: a critical assessment of recent developments on process fundamentals, models and applications, Desalination, 434 (2018) 121–160.
[16] M. Hayashi, Temperature-electrical conductivity relation of water for environmental monitoring and geophysical data inversion, Environ. Monit. Assess., 96 (2004) 119–128.
[17] A. Doyen, C. Roblet, L. Beaulieu, L. Saucier, Y. Pouliot, L. Bazinet, Impact of water splitting phenomenon during electrodialysis with ultrafiltration membranes on peptide selectivity and migration, J. Membr. Sci., 428 (2013) 349–356.